



Influence of laser photobiomodulation upon connective tissue remodeling during wound healing

Alena P. Medrado^{a,*}, Ana Prates Soares^a, Elisângela T. Santos^a, Sílvia Regina A. Reis^b, Zilton A. Andrade^a

^a Laboratory of Experimental Pathology, Oswaldo Cruz Foundation, Rua Waldemar Falcão, 121, Salvador, Bahia 40.296-710, Brazil

^b Department of Propaedeutics and Integrated Clinic, School of Dentistry, Federal University of Bahia, Rua Araújo Pinho 63, Salvador, BA 40.110-150, Brazil

ARTICLE INFO

Article history:

Received 2 November 2007

Accepted 19 May 2008

Available online 7 July 2008

Keywords:

Low level laser

Collagen

Silica

Fibrosis

ABSTRACT

The modulation of collagen fibers during experimental skin wound healing was studied in 112 Wistar rats submitted to laser photobiomodulation treatment. A standardized 8 mm-diameter wound was made on the dorsal skin of all animals. In half of them, 0.2 ml of a silica suspension was injected along the border of the wound in order to enhance collagen deposition and facilitate observation. The others received saline as vehicle. The treatment was carried out by means of laser rays from an aluminum-gallium arsenide diode semiconductor with 9 mW applied every other day (total dose = 4 J/cm²) on the borders of the wound. Tissue sections obtained from four experimental groups representing sham-irradiated animals, laser, silica and the association of both, were studied after 3, 7, 10, 15, 20, 30 and 60 days from the laser application. The wounded skin area was surgically removed and submitted to histological, immunohistochemical, ultrastructural, and immunofluorescent studies. Besides the degree and arrangement of collagen fibers and of their isotypes, the degree of edema, the presence of several cell types especially pericytes and myofibroblasts, were described and measured. The observation of Sirius-red stained slides under polarized microscopy revealed to be of great help during the morphological analysis of the collagen tissue dynamic changes. It was demonstrated that laser application was responsible for edema regression and a diminution in the number of inflammatory cells ($p < 0.05$). An evident increase in the number of actin-positive cells was observed in the laser-treated wounds. Collagen deposition was less than expected in silica-treated wounds, and laser treatment contributed to its better differentiation and modulation in all irradiated groups. Thus, laser photobiomodulation was able to induce several modifications during the cutaneous healing process, especially in favoring newly-formed collagen fibers to be better organized and compactly disposed.

© 2008 Elsevier B.V. All rights reserved.

1. Introduction

Several studies have recently demonstrated that laser photobiomodulation is able to alter cellular metabolism, especially by interfering with mitochondrial-membrane potential and ATP synthesis [1,2]. Furthermore, such modality of laser therapy is also effective in stimulating the cellular cycle and therefore cellular proliferation [3]. Through such capability of biostimulation, laser therapy may induce a decisive impact on the course of biological events that take place during wound healing. The gradual fibroblastic proliferation and the amount of collagen being synthesized can be particularly affected during tissue reconstruction [4]. Several exogenous factors may interfere with the structural pattern and the amount of collagen fibers being deposited during the heal-

ing process. Pugliese et al. [5] observed that skin wound experimentally produced in rats exhibited more collagen deposition when under low level laser irradiation, than the non-irradiated controls. An important detail about collagen bio-synthesis under laser irradiation has been stressed by Garavello-Freitas et al. [6]. They studied the structural pattern of the collagen fibers during bone repair by polarizing-light microscopy and observed that laser therapy induced the formation of more compact and paralleled-disposed fibers. Also, Fung et al. [7] experimentally demonstrated that collagen fibers appeared thicker and better organized in the collateral-medial ligaments of the knee, 3–6 weeks following surgery, supplemented by a 660 nm wavelength laser application.

The present study was aimed at investigating the interference of low level aluminum-gallium-arsenide laser upon collagen synthesis and its further structural organization during skin wound healing in rats. To better observe such changes by enhancing collagen production, two groups of rats were additionally injected with silica along the line demarcating the area of the skin that should be immediately removed.

* Corresponding author. Tel.: +55 71 31762266; fax: +55 71 31762345.

E-mail addresses: alenamedrado@hotmail.com (A.P. Medrado), prates_ana@hotmail.com (A.P. Soares), elistrin@hotmail.com (E.T. Santos), srareis@uol.com.br (S.R.A. Reis), zilton@bahia.fiocruz.br (Z.A. Andrade).

2. Materials and methods

2.1. Experimental groups

One hundred and twelve Wistar rats of both sexes, weighing 220 g, were kept in individual cages with good conditions of light and room temperature ($\pm 26^{\circ}\text{C}$), with free access to a balanced commercial diet. All the animals had their dorsal skin shaved and cleaned. In the center of this shaved area an 8 mm-diameter circle was marked with India ink. This marked area was either injected with 0.2 ml of saline for half of the animals or with 0.2 ml of a silica suspension for the remaining half (approximately 3×10^6 particles, calculated with the use of a hemocytometer). Injections were made around the inner periphery from the ink-demarcated circle, into four points of the superficial dermis, under strict conditions of asepsis and anesthesia. Three days afterwards, a circular portion of the skin was removed from the delimited area of all animals by means of an 8 mm-diameter circular device (Biopsy Punch – Stiefel – Germany), leaving a well delimited and uniform skin ulcer, which was thereafter investigated.

The animals were divided into four experimental groups.

2.1.1. Group I

Sham-irradiated controls with the skin ulcer produced in an area previously injected with saline.

2.1.2. Group II

Laser, animals with the skin ulcer produced in an area previously injected with saline and submitted to low level laser irradiation, as follows: a semi-conductor diode As–Ga–Al laser apparatus was used to deliver a 9 mW–670 nm wavelength treatment (Laser VR-KC-610 Dentoflex, Brazil). Four 0.5 J/cm^2 punctual applications were performed on the edges of the wound so that the total dose of 1 J/cm^2 was reached every other day, until a dose of 4 J/cm^2 was completed. Time used for the laser-ray application of each point was based on an equation proposed by Tuner and Hode [8], which indicated 31 s per session. The total time corresponding to 4 J/cm^2 of energy density was 124 s. To estimate the area at the light beam emission point, a specimenter provided with a scale from 0.1 to 10 mm^2 was used. The area of the spot size was $28.27 \times 10^{-2} \text{ cm}^2$ and power density about 31 mW/cm^2 . The dose of 4 J/cm^2 was selected on the basis of previous studies by Medrado et al. [9].

2.1.3. Group III

Silica, animals from this group were injected with silica 3 days before the skin ulcer was produced and treated in the same way as for the others groups, but with the laser apparatus unplugged.

2.1.4. Group IV

Laser + silica, animals from this group were injected with silica 3 days before the skin ulcer was produced and submitted to low level laser irradiation. Laser therapy was similar to that of the previous group II.

Upon completing the laser treatment, tissues representative of the border of the ulcer were removed from all the experimental animals at 3, 7, 10, 15, 20, 30 and 60 days post treatment, and immediately submitted to the following procedures. Four animals of each group were killed at these specific days.

2.2. Histology

Fragments of the skin, including the margin of the wound and subcutaneous tissue were fixed in 10% neutral formalin, followed by paraffin embedding, and the microtome sections were stained

with hematoxilyn and eosin and Sirius-red. The cuts stained with picrosirius were examined under a polarized light microscope and analysis of the results obtained from the examination of the sections was descriptively expressed. Changes affecting the number of polymorphonuclear inflammatory cells, the degree of edema, mononuclear inflammatory cells and collagen fibers deposition were semi-quantitatively and blindly evaluated in coded slides and registered as absent (0), mild (+), moderate (++) and marked (+++).

2.3. Fluorescence microscopy

Fragments of the ulcerated skin were immediately placed in Tissue-Tek, and immersed into liquid nitrogen for a few minutes and kept frozen at -70°C in airtight boxes, until the moment they were sectioned in a cryostat at -20°C . The sections were submitted to an indirect immunofluorescence technique for the demonstration of collagen isotypes (I, III and IV), laminin and fibronectin. The specific anti-sera were polyclonal, obtained in rabbits (Institute Pasteur, France). They were used in dilution varying from 1:40 to 1:100. Details concerning their preparation and tests of specificity appeared elsewhere [10]. Secondary fluoresceinated anti rabbit IgG was commercially obtained from Sigma, USA and diluted at 1:40 in PBS with 2% of BSA diluted at 1/5 in Evans' blue. Analyses of the results obtained from the examination of the sections were descriptively expressed.

2.4. Immunohistochemistry

For the demonstration of SM- α actin and desmin, paraffin sections of formalin-fixed tissue were used. Antigen retrieval was accomplished through micro-wave treatment in citrate buffer at pH 6.0. Sections were incubated with the primary antibodies either for anti-alpha-1 actin (1:800; clone 1A4) or anti-desmin (1:100; clone M0760) overnight, at 4°C in a humidified chamber (DAKO, Carpinteria, CA, USA). Primary antibodies were diluted in 2% BSA in PBS (pH 7.4). After washing in PBS, sections were incubated in 10% skimmed milk during 20 min for blocking non-specific ligations. The slides were then incubated with the secondary antibody: a sheep – anti-Rat IgG conjugated to peroxidase (Dako envision system – labeled polymer, Dako, USA) at the dilution of 1:1000 for 30 min at 37°C in an humidified chamber. Blockage of the endogenous peroxidase was done with 0.3% H_2O_2 for 30 min, at room temperature. The color was developed with 0.06% 3,3'-diaminobenzidine tetrahydrochloride (DAB) (Sigma, St. Louis, Mo-USA) and 0.06% H_2O_2 plus 1% dimethylsulphoxide (Sigma, St. Louis, Mo-USA). Sections were counterstained with 1% hematoxilyn for 5 min, dehydrated and mounted with Permount. Control sections in which primary antibody was either omitted or replaced by normal mouse serum diluted in 1:300 were used as negative controls. Positive controls were obtained of smooth muscle of a rat's uterus for anti-alpha-1 actin and stried muscle for anti-desmin. Changes affecting the number of cells marked for desmin and smooth muscle alpha actin were semi-quantitatively evaluated in accordance with the same parameters described in histology section.

2.5. Transmission electron microscopy

Tiny fragments of the skin (about 1 mm^3) were immediately fixed by immersion into 4% glutaraldehyde in 0.2 M cacodylate buffer, pH 7.4, for 1 h at 4°C , washed in buffer and postfixed with 1% osmium tetroxide, dehydrated in graded concentrations of acetone and embedded in Poly-bed 812 (Embedding Media Polysciences, IVC). Selected ultrathin sections (50–70 nm) were made with a Reichert (Ultratome Supernova Leica) ultramicrotome and mounted on uncoated copper grids, contrasted with uranyl acetate

and a lead citrate. Specimens were examined in a Zeiss EM-9 electron microscope, which was operated at an acceleration voltage of 50 kV. The sections were also descriptively expressed.

2.6. Statistical analysis

A non-parametric version of the Exact Kruskal–Wallis test for the determination of differences between groups was used, together with the Dunn's multiple comparison test for pair analysis. Results were considered significant when reached $p < 0.05$.

3. Results

3.1. Group I

In the histological sections stained with hematoxylin and eosin of sham group, corresponding to the third day after surgical procedure, accentuated edema and marked inflammatory infiltrate of predominantly neutrophilic polymorphonuclear cells were observed (Fig. 1, Tables 1 and 3). Mild lymphocytic infiltrate were seen (Table 2). In some areas, the sections observed under polarized light showed a predominance of greenish-yellow fibers with irregular refraction. On the seventh day, it was observed that all sham and irradiated animals exhibited granulation tissue, with angiogenesis and increased mononuclear cell infiltrate, especially macrophages and lymphocytes (Table 2). Collagen matrix under polarized light showed a predominance of greenish-yellow fibers,

and few thick yellowish-orange fibers disposed in various directions were observed. The content of collagen was always less expressive when compared to the other groups. The difference was even greater at the 10th day (Fig. 5A, Table 6). The presence of cells expressing alpha actin and desmin was discrete at different periods of death. The immunofluorescence findings revealed mild expression of collagen and fibronectin, which was confirmed by ultrastructural study. Although this group exhibited a delayed wound healing, all the animals showed similar histological characteristics at the final periods of the experiment.

3.2. Group II

The earliest microscopical changes observed in the skin wounds in all groups were dominated by acute inflammation, but from the 3rd day on those changes subsided, and were gradually replaced by mononuclear leukocytes. However, the laser-irradiated animals exhibited much less polymorphonuclear cells than their respective controls (Table 1). Infiltration of small islets of adipose cells were observed in the dermis (Fig. 1B). Mononuclear infiltrate was statistical different from the others groups at this time (Table 2). Seven days after the wound was inflicted, all the groups presented a prominent granulation tissue which became more and more evident, with the sprouting of numerous small blood capillaries accompanied by disperse fusiform cells and edema. Edema decreased significantly in the laser-treated group, as can be appreciated in Table 3. The granulation tissue was made particularly

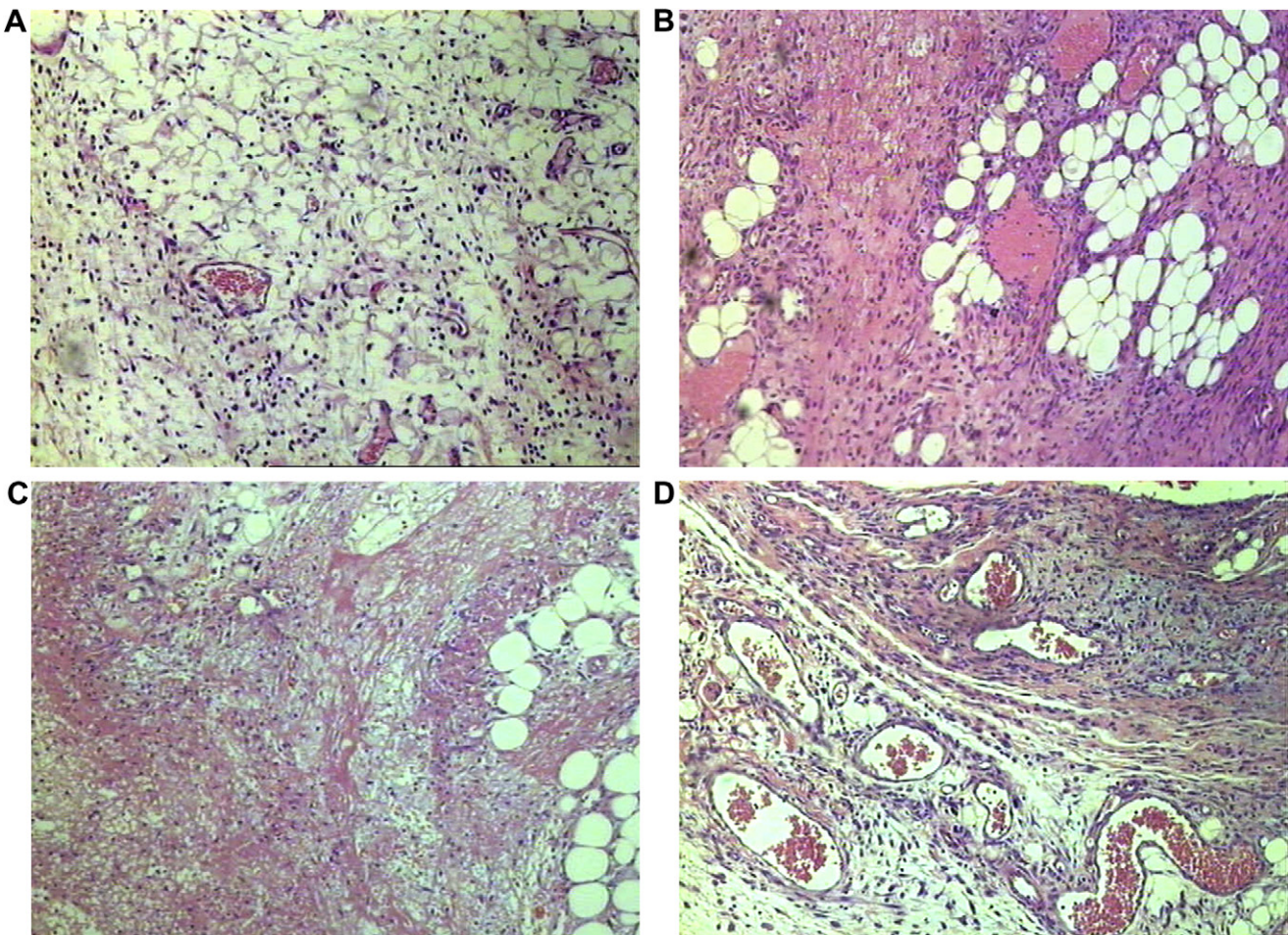


Fig. 1. Presence of edema and inflammatory infiltrate as observed in different experimental groups three days after the surgical procedure. (A) Control; (B) laser; (C) silica; (D) laser/silica. Hematoxilyn–eosin staining, X100.

evident when the sections treated with a fluoresceinated anti-laminin serum were observed under U-V light, especially for the laser-treated group (Fig. 2). This group also presented several scattered fusiform smooth-muscle alpha-actin positive cells, both around the proliferating capillaries and venules, as in the interior of the inflammatory tissue (Table 4, Figs. 3 and 4). In addition anti-desmin positive cells appeared sparse within granulation tissue (Table 5). Around the 10th day the general pattern differed little from the above described. However, the lesions submitted to laser irradiation exhibited a diminution in the degree of edema, which became mild. Also, they disclosed mild, but significant differences in the amount and in distribution pattern, regarding the collagen fibers, which appeared straight instead of wavy, thicker and with a tendency toward a parallel disposition, as compared to non-irradiated wounds (Table 6, Fig. 5B). Fluorescence microscopy revealed a gradual increase of type I collagen and fibronectin, especially prominent in the animals submitted to silica contamination and laser treatment. At this point, the electron microscopical picture was compatible with and increased synthesis activity, as demonstrated by the presence of fibroblasts and myofibroblasts with proliferated and dilated endoplasmic reticulum, in the middle of collagen fibrils and abundant amorphous material (proteoglycans), and mild edema (Figs. 6 and 7).

3.3. Group III

As for the silica-injected group fibrinous exsudation represented a prominent change, regardless of laser treatment (Fig.

1C). The areas just below the crust and little above the muscular layer were particularly involved. Under the electron microscope such deposit appeared structureless with a tendency to form small aggregations (Fig. 8). During this early stage collagen fibers and fibrils were thin, bent and distributed at random, without a particular spatial orientation. They acquire a greenish hue when viewed under polarized light. However, they tend to form thicker bundles at the 10th day (Fig. 5C), although the expression of total collagen was always smaller than that of the other experimental groups at different days of death. Fluorescence microscopy exhibited a gradual increase of type I collagen similar to Group II. Fibronectin was also seen in focal areas of inflammatory exudate which was observed until the 10th day. Sections from the silica group revealed in addition focal collection of polymorphonuclear leukocytes (Table 1) and foreign body giant cells, besides a strong proliferation of fusiform basophilic cells and blood capillaries (angiogenesis). The silica treated group allowed for an enhancement of chronic inflammation in the wounds (Table 2). Another prominent finding was the presence of alpha-actin positive cells at 20, 30 and 60th days.

3.4. Group IV

On the third day large ectatic and congested vessels were evident (Fig. 1D). Edema and polymorphonuclear leukocytes were mild and at this time of death, a large contingent of mononuclear cells were noted, especially macrophages and lymphocytes (Tables 1–3). On the seventh day, the granulation tissue formation was

Table 1

Distribution of the polymorphonuclear cells in the sham, laser, silica and laser/silica treated groups

Time of death (days)	Group	Median	Q ₁ –Q ₃ ^g	p
3	Sham	3.00	2.25–3.00	0.029*
	Laser	2.00	2.00–2.00	
	Silica	3.00	2.25–3.00	
	Laser + silica	2.00	2.00–2.00	
7	Sham	1.00 ^{a,b,c}	1.00–1.00	0.002*
	Laser	0.00 ^{a,d}	0.00–0.00	
	Silica	1.00 ^{d,f}	1.00–1.00	
	Laser + silica	0.00 ^{b,f}	0.00–0.00	
10	Sham	1.00	0.25–1.00	0.016*
	Laser	0.00	0.00–0.00	
	Silica	0.00	0.00–0.00	
	Laser + silica	0.00	0.00–0.00	
15	Sham	0.00	0.00–0.00	1.000
	Laser	0.00	0.00–0.00	
	Silica	0.00	0.00–0.00	
	Laser + silica	0.00	0.00–0.00	
20	Sham	0.00	0.00–0.00	1.000
	Laser	0.00	0.00–0.00	
	Silica	0.00	0.00–0.00	
	Laser + silica	0.00	0.00–0.00	
30	Sham	0.00	0.00–0.00	1.000
	Laser	0.00	0.00–0.00	
	Silica	0.00	0.00–0.00	
	Laser + silica	0.00	0.00–0.00	
60	Sham	0.00	0.00–0.00	1.000
	Laser	0.00	0.00–0.00	
	Silica	0.00	0.00–0.00	
	Laser + silica	0.00	0.00–0.00	

* The median difference is significant at the 0.05 level.

^a Significant difference between sham and laser groups.

^b Significant difference between sham and silica groups.

^c Significant difference between sham and laser + silica groups.

^d Significant difference between laser and silica groups.

^e Significant difference between laser and laser + silica groups.

^f Significant difference between silica and laser + silica groups.

^g Q₁ – Lower quartiles/Q₃ – Upper quartiles.

Table 2

Distribution of the mononuclear cells in the sham, laser, silica and laser/silica treated groups

Time of death (days)	Group	Median	Q ₁ –Q ₃ ^g	p
3	Sham	2.00	2.00–2.75	0.172
	Laser	2.50	2.00–3.00	
	Silica	2.00	2.00–2.00	
	Laser + silica	3.00	2.25–3.00	
7	Sham	2.00	2.00–2.00	0.002*
	Laser	2.00	2.00–2.00	
	Silica	3.00 ^f	3.00–3.00	
	Laser + silica	1.00 ^f	1.00–1.00	
10	Sham	2.00	1.25–2.00	0.004*
	Laser	1.00	0.25–1.00	
	Silica	2.00 ^f	2.00–2.00	
	Laser + silica	0.00 ^f	0.00–0.00	
15	Sham	2.00 ^a	2.00–2.00	0.002*
	Laser	0.00 ^a	0.00–0.00	
	Silica	1.00	1.00–1.00	
	Laser + silica	1.00	1.00–1.00	
20	Sham	0.00 ^c	0.00–0.00	0.007*
	Laser	0.00 ^e	0.00–0.00	
	Silica	1.00	0.25–1.00	
	Laser + silica	1.00 ^{c,e}	1.00–1.00	
30	Sham	0.00 ^c	0.00–0.00	0.008*
	Laser	0.00 ^e	0.00–0.00	
	Silica	0.00	0.00–0.75	
	Laser + silica	1.00 ^{c,e}	1.00–1.00	
60	Sham	0.00	0.00–0.75	0.392
	Laser	0.00	0.00–0.00	
	Silica	0.00	0.00–0.00	
	Laser + silica	0.00	0.00–0.00	

* The median difference is significant at the 0.05 level.

^a Significant difference between sham and laser groups.

^b Significant difference between sham and silica groups.

^c Significant difference between sham and laser + silica groups.

^d Significant difference between laser and silica groups.

^e Significant difference between laser and laser + silica groups.

^f Significant difference between silica and laser + silica groups.

^g Q₁ – Lower quartiles/Q₃ – Upper quartiles.

more expressive than those of sham and silica groups, but was very similar to laser group. The same aspect was observed as far as concerned to alpha actin and desmin positive cells. Ultrastructurally, fibroblasts were more frequent in comparison to the silica group and exhibited a slightly more developed rough endoplasmatic

reticulum. Deposition of denser matrix was verified, and next to the fibroblasts, collagen fibers exhibiting packed and organized appearance were observed. At the 10th day, the collagenous matrix was constituted of fibers of varying thickness, with a more evident organizational pattern than those observed in the sham and silica

Table 3
Distribution of edema in the sham, laser, silica and laser/silica treated groups

Time of death (days)	Group	Median	$Q_1-Q_3^g$	p
3	Sham	3.00 ^a	3.00–3.00	0.002*
	Laser	2.00 ^{a,d}	2.00–2.00	
	Silica	3.00 ^{d,f}	3.00–3.00	
	Laser + silica	2.00 ^f	2.00–2.00	
7	Sham	1.00 ^c	1.00–1.00	0.025*
	Laser	0.00	0.00–0.75	
	Silica	1.00	0.25–1.00	
	Laser + silica	0.00 ^c	0.00–0.00	
10	Sham	2.00 ^{a,b,c}	1.25–2.00	0.002*
	Laser	0.00 ^a	0.00–0.00	
	Silica	0.00 ^b	0.00–0.00	
	Laser + silica	0.00 ^c	0.00–0.00	
15	Sham	0.00	0.00–0.00	1.000
	Laser	0.00	0.00–0.00	
	Silica	0.00	0.00–0.00	
	Laser + silica	0.00	0.00–0.00	
20	Sham	0.00	0.00–0.00	1.000
	Laser	0.00	0.00–0.00	
	Silica	0.00	0.00–0.00	
	Laser + silica	0.00	0.00–0.00	
30	Sham	0.00	0.00–0.00	1.000
	Laser	0.00	0.00–0.00	
	Silica	0.00	0.00–0.00	
	Laser + silica	0.00	0.00–0.00	
60	Sham	0.00	0.00–0.00	1.000
	Laser	0.00	0.00–0.00	
	Silica	0.00	0.00–0.00	
	Laser + silica	0.00	0.00–0.00	

* The median difference is significant at the 0.05 level.

^a Significant difference between sham and laser groups.

^b Significant difference between sham and silica groups.

^c Significant difference between sham and laser + silica groups.

^d Significant difference between laser and silica groups.

^e Significant difference between laser and laser + silica groups.

^f Significant difference between silica and laser + silica groups.

^g Q_1 – Lower quartiles/ Q_3 – Upper quartiles.

Table 4
Distribution of alpha-actin positive cells in the sham, laser, silica and laser/silica treated groups

Time of death (days)	Group	Median	$Q_1-Q_3^g$	p
3	Sham	1.00 ^c	1.00–1.00	0.002*
	Laser	1.00 ^e	1.00–1.00	
	Silica	2.00	2.00–2.00	
	Laser + silica	3.00 ^{c,e}	3.00–3.00	
7	Sham	1.00 ^{b,c}	1.00–1.00	0.008*
	Laser	3.00	1.50–3.00	
	Silica	3.00 ^b	3.00–3.00	
	Laser + silica	3.00 ^c	3.00–3.00	
10	Sham	1.00 ^{b,c}	1.00–1.00	0.008*
	Laser	2.00	1.25–2.00	
	Silica	2.00 ^b	2.00–2.00	
	Laser + silica	2.00 ^c	2.00–2.00	
15	Sham	1.00	1.00–1.00	1.000
	Laser	1.00	1.00–1.00	
	Silica	1.00	1.00–1.00	
	Laser + silica	1.00	1.00–1.00	
20	Sham	0.50	0.00–1.00	0.093
	Laser	1.00	1.00–1.00	
	Silica	1.00	1.00–1.00	
	Laser + silica	1.00	1.00–1.00	
30	Sham	0.00 ^{a,b,c}	0.00–0.00	0.002*
	Laser	1.00 ^a	1.00–1.00	
	Silica	1.00 ^b	1.00–1.00	
	Laser + silica	1.00 ^c	1.00–1.00	
60	Sham	0.00	0.00–0.00	0.058
	Laser	0.50	0.00–1.00	
	Silica	1.00	1.00–1.00	
	Laser + silica	0.50	0.00–1.00	

* The median difference is significant at the 0.05 level.

^a Significant difference between sham and laser groups.

^b Significant difference between sham and silica groups.

^c Significant difference between sham and laser + silica groups.

^d Significant difference between laser and silica groups.

^e Significant difference between laser and laser + silica groups.

^f Significant difference between silica and laser + silica groups.

^g Q_1 – Lower quartiles/ Q_3 – Upper quartiles.

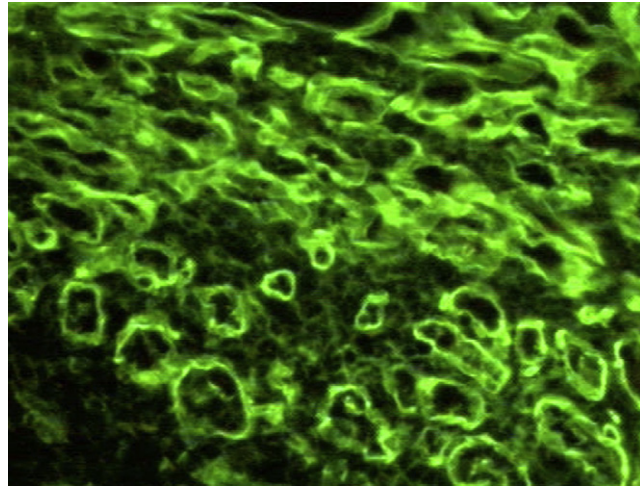


Fig. 2. Fluorescent basement membrane from proliferated blood vessels appears in a three-day wound made in a laser group animal. Immuno-fluorescence anti-laminin staining, X200.

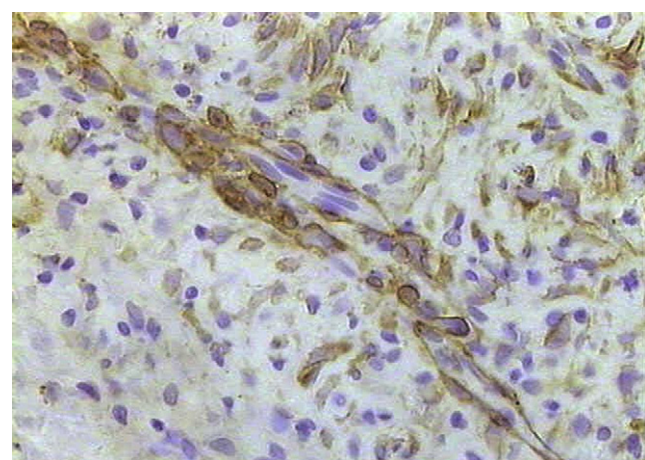


Fig. 3. Fusiform smooth-muscle alpha-actin positive cells around the proliferating capillaries and venules. Endothelial cells appear unmarked. Laser group, 7 days. Immunohistochemistry, smooth-muscle alpha-actin, X400.

groups, showing a larger contingent of thicker, yellow-orange fibers. Total collagen was greater for the laser irradiated groups (**Table 6**), but some differences were noted in the distribution and appearance of the collagen fibers during electron microscope examination, even when laser/silica animals and non-irradiated

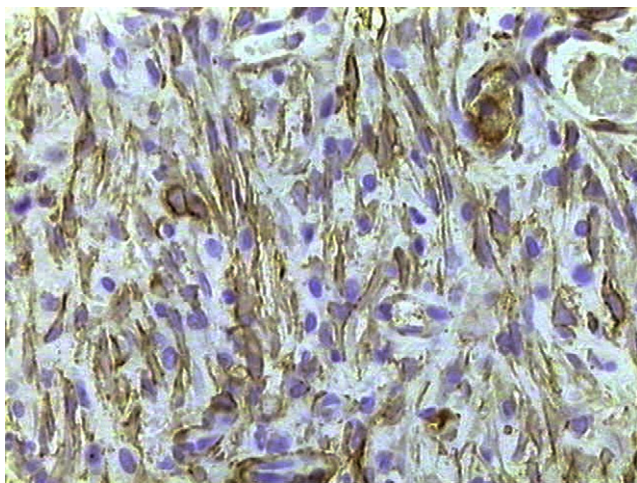


Fig. 4. Fusiform smooth-muscle alpha-actin positive cells in the middle of the inflammatory tissue. Silica group, 7 days. Immunohistochemistry, smooth-muscle alpha-actin, X400.

Table 5
Distribution of desmin positive cells in the sham, laser, silica and laser/silica treated groups

Time of death (days)	Group	Median	Q ₁ –Q ₃ ^g	p
3	Sham	0.00	0.00–0.75	0.010*
	Laser	0.00	0.00–0.75	
	Silica	2.00	1.25–2.00	
	Laser + silica	2.00	1.25–2.00	
7	Sham	0.00 ^e	0.00–0.00	0.011*
	Laser	1.00	0.25–1.00	
	Silica	1.00	1.00–1.00	
	Laser + silica	1.00 ^e	1.00–1.75	
10	Sham	1.00	1.00–1.00	0.238
	Laser	1.00	0.25–1.00	
	Silica	0.50	0.00–1.00	
	Laser + silica	1.00	1.00–1.00	
15	Sham	1.00 ^c	1.00–1.00	0.040*
	Laser	0.00	0.00–0.75	
	Silica	0.50	0.00–1.00	
	Laser + silica	0.00 ^c	0.00–0.00	
20	Sham	0.50	0.00–1.00	0.093
	Laser	0.00	0.00–0.00	
	Silica	0.00	0.00–0.00	
	Laser + silica	0.00	0.00–0.00	
30	Sham	0.00	0.00–0.00	1.000
	Laser	0.00	0.00–0.00	
	Silica	0.00	0.00–0.00	
	Laser + silica	0.00	0.00–0.00	
60	Sham	0.00	0.00–0.00	1.000
	Laser	0.00	0.00–0.00	
	Silica	0.00	0.00–0.00	
	Laser + silica	0.00	0.00–0.00	

* The median difference is significant at the 0.05 level.

^a Significant difference between sham and laser groups.

^b Significant difference between sham and silica groups.

^c Significant difference between sham and laser + silica groups.

^d Significant difference between laser and silica groups.

^e Significant difference between laser and laser + silica groups.

^f Significant difference between silica and laser + silica groups.

^g Q₁ – Lower quartiles/Q₃ – Upper quartiles.

ones were compared. In the former, collagen fibers were longer, parallel and straight, while in the latter they tended to appear fragmented and less uniform in thickness (**Figs. 9 and 10**). Collagen type III predominated in the first days of healing, but its expression decreased rapidly as the expression of collagen type I became more evident from the 7th day on. Sixty days elapsed from surgery, the wounds from all the groups tended to acquire a more uniform appearance, the wound area becoming a depressed fibroplastic plaque covered by skin with a thin epidermis and absence of follicles in the fibrotic dermis. No appreciable differences could be registered when the wounds from all groups were compared at this final period.

4. Discussion

The present investigation revealed once more that laser therapy has the ability to incite some biological phenomena capable of modulating the morphological pattern of the connective tissue during repair and healing. The animals with experimental skin ulcers that were submitted to laser treatment presented statistically significant reduction of the amount of edema and the degree of polymorphonuclear leukocyte exudates, 3–7 days following laser application. Similar findings have been described in the literature [11]. Thus, the accumulated data are in accordance with the idea that laser treatment depresses the exudative phase at the same time that enhances the proliferative processes during acute and chronic inflammation.

Table 6
Distribution of the collagen in the sham, laser, silica and laser/silica treated groups

Time of death (days)	Group	Median	Q ₁ –Q ₃ ^g	p
3	Sham	0.00	0.00–0.75	0.016*
	Laser	1.00	1.00–1.00	
	Silica	1.00	1.00–1.00	
	Laser + silica	1.00	1.00–1.00	
7	Sham	1.00	1.00–1.00	0.058
	Laser	1.00	1.00–1.00	
	Silica	1.00	1.00–1.75	
	Laser + silica	2.00	1.25–2.00	
10	Sham	1.00	1.00–1.75	0.028*
	Laser	2.00	2.00–2.00	
	Silica	1.00	1.00–1.75	
	Laser + silica	2.00	2.00–2.75	
15	Sham	2.00	2.00–2.75	0.172
	Laser	3.00	2.25–3.00	
	Silica	2.00	2.00–2.00	
	Laser + silica	2.50	2.00–3.00	
20	Sham	3.00	2.25–3.00	0.008*
	Laser	3.00 ^d	3.00–3.00	
	Silica	2.00 ^{d,f}	2.00–2.00	
	Laser + silica	3.00 ^f	3.00–3.00	
30	Sham	3.00	3.00–3.00	0.016*
	Laser	3.00	3.00–3.00	
	Silica	2.00	2.00–2.75	
	Laser + silica	3.00	3.00–3.00	
60	Sham	3.00	3.00–3.00	0.392
	Laser	3.00	3.00–3.00	
	Silica	3.00	2.25–3.00	
	Laser + silica	3.00	3.00–3.00	

* The median difference is significant at the 0.05 level.

^a Significant difference between sham and laser groups.

^b Significant difference between sham and silica groups.

^c Significant difference between sham and laser + silica groups.^d Significant difference between laser and silica groups.

^e Significant difference between laser and laser + silica groups.

^f Significant difference between silica and laser + silica groups.

^g Q₁ – Lower quartiles/Q₃ – Upper quartiles.

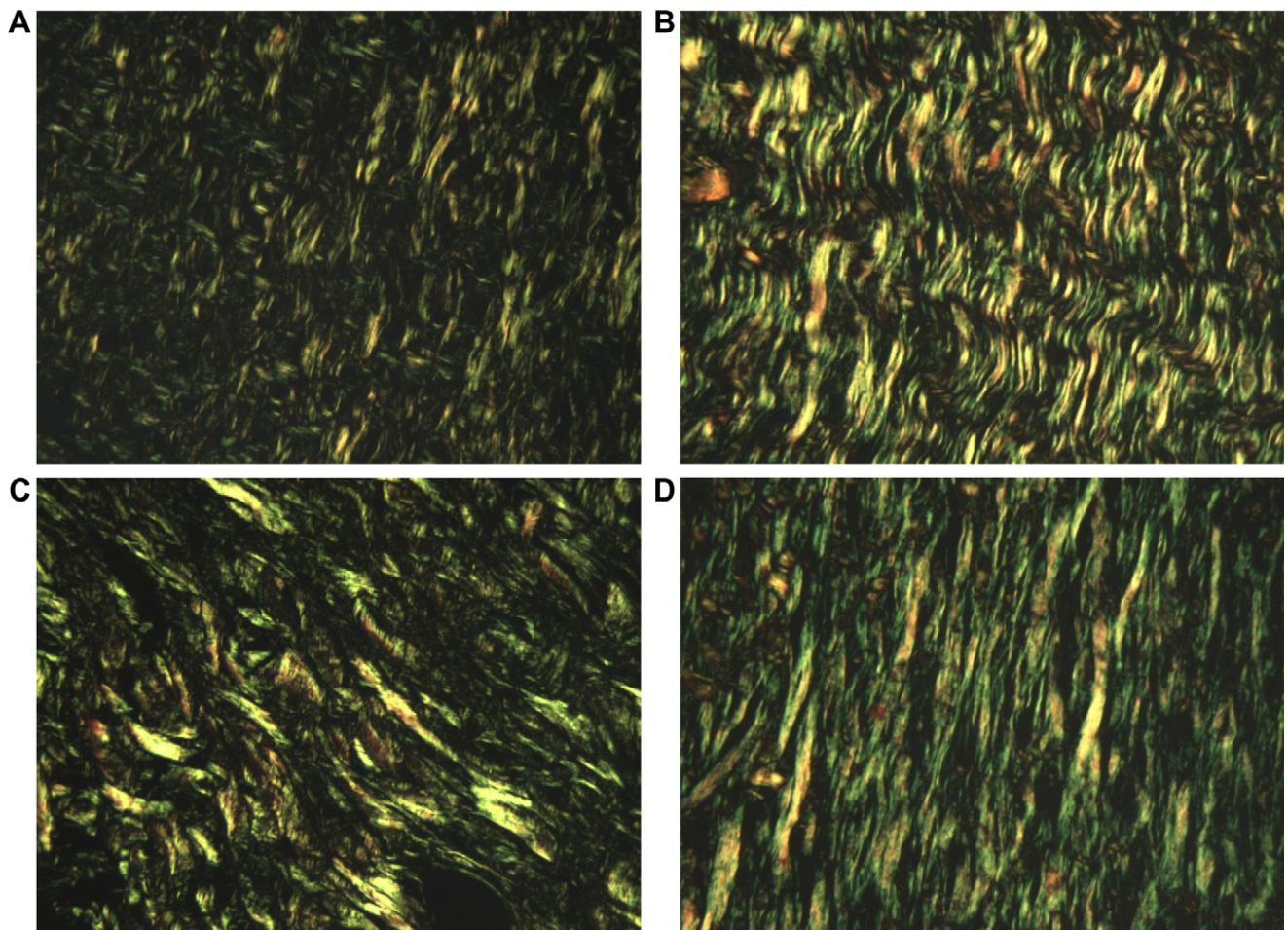


Fig. 5. Collagen fiber pattern observed under polarized light in different experimental groups ten days after the surgical procedure. (A) Control; (B) laser; (C) silica; (D) laser/silica. Picosirius staining, X400.

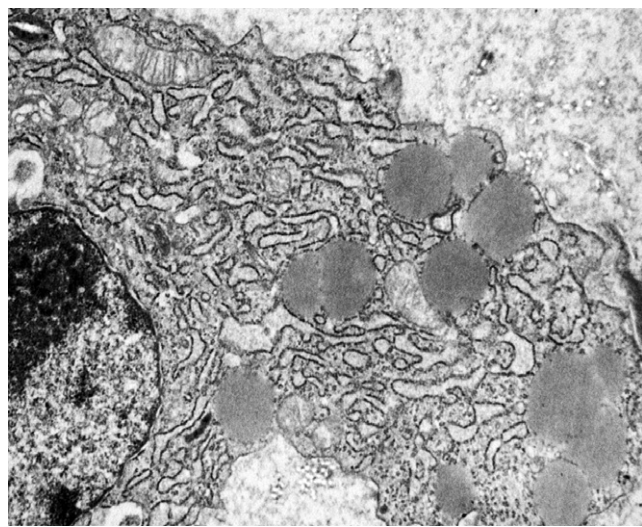


Fig. 6. A fibroblast exhibiting hyperplastic and dilated endoplasmic reticulum and fatty vacuoles from a laser group animal, 10th day. Electron micrograph, X12 000.

It is known that silica is an important fibrosis inductor. It has been observed that silica stimulates collagen synthesis by fibroblasts [12,13]. The evidences indicate that biological products secreted by macrophages during phagocytosis of silica particles,

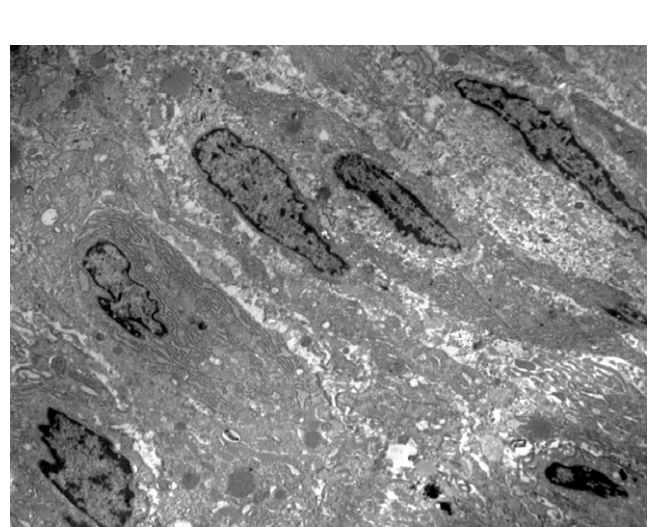


Fig. 7. A group of fibroblasts aligned on the extracellular matrix of an animal treated with laser, 10th day. Electron micrograph, X4 400.

such as TGF- β , are able to stimulate the deposition of collagenous matrix locally [14]. Similarly, data from the literature also refer that low-level laser increases collagen contents in extracellular matrix [5]. Of course the increase in the amount of collagen fibrils

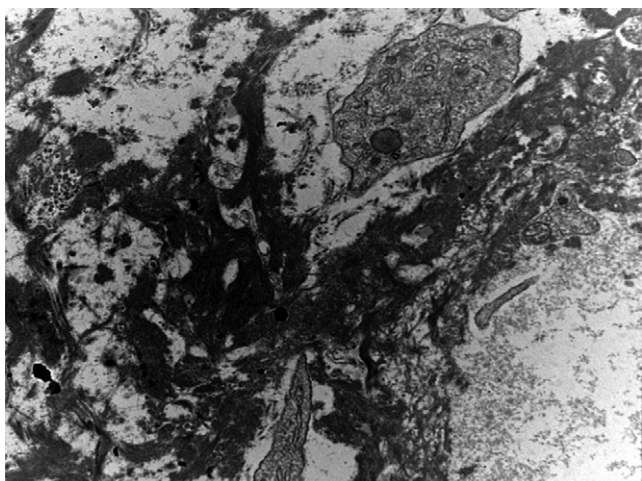


Fig. 8. Fibrin deposits appear within the extracellular matrix. Silica-treated animal, three days after the wound was inflicted. Electron micrograph, X7 000.

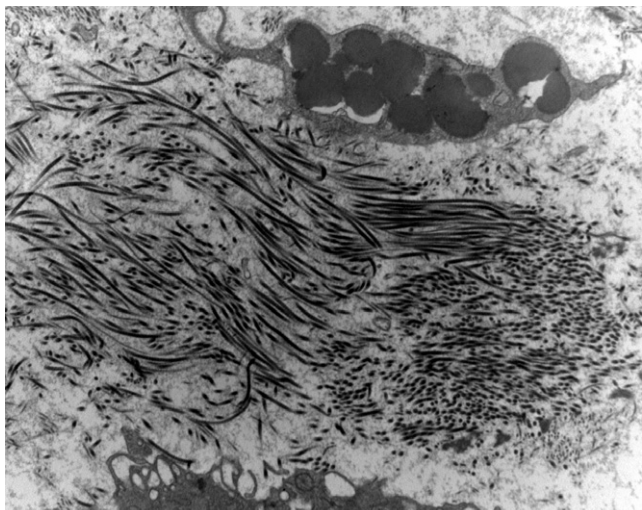


Fig. 9. An irregular distribution of collagen fibers as seen in an animal from silica group without laser irradiation, 10 days. Electron micrograph, X7 000.

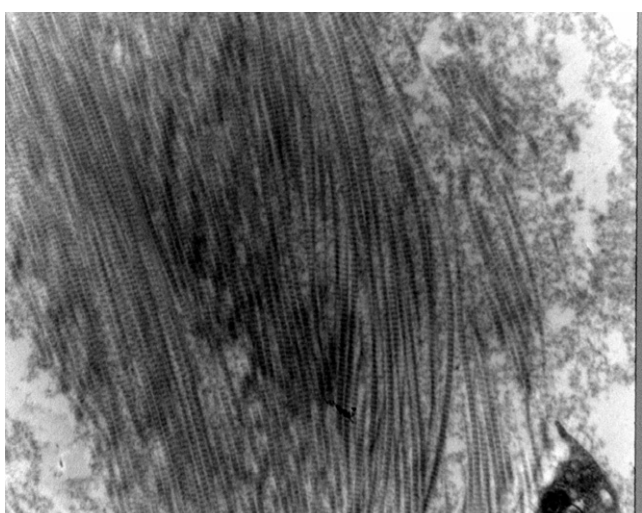


Fig. 10. Collagen fibers appear more compactedly arranged in a laser/silica-treated animal. 10 days. Electron micrograph, X7 000.

and fibers in the matrix during laser treatment may result from a combination of fibroblast proliferation coupled to enhanced collagen synthesis by such cells. Therefore, laser may act by stimulating either or both ways at the same time.

The addition of silica to the inflicted skin wound, as was made in two groups of rats, was used as an experimental tool in order to increase collagen production, and thus facilitate the observation of the changes that laser treatment would bring about. However, the comparative analysis of the silica groups at 15, 20, 30 and 60 days did not demonstrate significant differences in the rate of collagen deposition when compared with their respective controls. The increase in collagen deposition was less than expected, and did not result in much additional information during the microscopic studies. Probably one of the reasons for that was connected to the physical state of the silica being used. It has been demonstrated that recently fractured silica is more fibrogenic than that kept in bottles for a prolonged time [15].

Ultrastructural findings from the silica-treated groups frequently exhibited deposits of structureless amorphous material within the interstitial tissue, sometimes forming small focal accumulations, probably fibrin-derived. According to Giorgio-Miller et al. [16] fibrin from the interstitial fluid may induce fibrosis in the mouse skin lacking the plasminogen-activate factor. Although a large amount of this insoluble protein was observed at the early stages of the repair process in silica-treated rats, the statistical analysis of collagen was not significant between sham and silica groups.

Microscopic observation under polarizing light was proved adequate for the qualitative analysis, due to the birefringence of collagen fibers and fibrils. Such birefringence reveals a supramolecular organization, with macromolecules arranged in parallel fashion. Besides collagen, actin (F-actin), myosin, and intermediate filaments may also disclose birefringence [17,18]. Modulation during repair, leading to the appearance of more compacted and parallel-oriented collagen fibers, can result in the formation of a structure similar to that of the lost original tissue, including the reestablishment of the tensile force. These features were here demonstrated in the animals subjected to laser treatment at 10, 15 and 20 days from the skin wound, when thicker parallel collagen fibers replaced the damaged area. Fluorescence microscopy analyses revealed a tendency of earlier substitution of collagen type III by type I in laser treated animals. However, from the 30th day on such difference was less apparent, since collagen tissue replacement from all groups similarly showed the same advanced degree of maturation.

Immunohistochemistry with anti-alpha actin antibody has currently been used to mark smooth muscle, and to identify myofibroblasts and pericytes [19,20]. Medrado et al. [9] have demonstrated the presence of great number of actin-positive cells in rats with 3–7-day-old experimental skin ulcers following treatment with laser. Ultrastructural findings confirmed the immunohistochemical data by revealing myofibroblasts as fusiform cells, with hyperplastic rough endoplasmic reticulum, indented nuclei, and perinuclear basement-membrane-like material. These results were also reported by others [21]. In the present investigation the number of actin-positive cells was even more significant for the irradiated groups at the 3, 7 and 10 days, although the non-irradiated silica-treated group, also revealed similar findings at the 3rd day when compared to controls. Several of these actin-positive cells showed para-vasal position, and some of them appeared to be detaching from the periphery of capillaries and venules. They were identified as pericytes, and appeared in great numbers in irradiated animals. The participation of pericytes during the healing process has already been described, and new functions have been described to these cells, especially suggesting the possibility that they may function as “reserve cells” or “stem-cells”. Although, the

plasticity and other properties of the pericytes are still in need of further studies, their potential to differentiate into osteoblasts, chondrocytes, fibroblasts, leiomyocytes and adipocytes has already been largely studied [22]. Probably the participation of pericytes in wound healing is still more important and fundamental than we can now imagine. Another prominent finding detected in the present study refers to angiogenesis. It has been recognized as an essential element in several physiological and pathological processes, such as embryogenesis and growth, healing, neoplasia, metastasis, and so on. The new microvasculature allows the exchange of fluids, oxygen, nutrients and cells within the stroma [23]. Laser photobiomodulation can activate the local blood circulation and stimulate proliferation of endothelial cells, as reported by some [24,25].

Immunofluorescent microscopy was of help in demonstrating collagen types (I and III), as well as fibronectin, within the healing tissues, although no clear cut differences were noted as far as their general pattern of distribution was concerned, except that fibronectin appeared more concentrated in focal inflammatory zones.

As herein reported, external factors such as laser and silica were identified as capable of modulating collagen synthesis during cutaneous wound healing, with increasing efficacy when both factors acted together. Moreover, laser irradiation, even when associated with silica, allowed a better arrangement of the collagen fibers arrangement, necessary for the development of the tensile force of the cicatricial tissue. Similar data confirm and support data that have been presented in relation to bone and ligament repair [6,7], all of them indicative that laser therapy play a decisive role in influencing the quality of the extracellular matrix during wound healing.

References

- [1] L. Gavish, Y. Asher, Y. Becker, Y. Kleinman, Low level laser irradiation stimulates mitochondrial membrane potential and disperses subnuclear promyelocytic leukemia protein, *Lasers Surg. Med.* 35 (2004) 369–376.
- [2] S. Passarella, E. Casamassima, S. Molinari, D. Pastore, E. Quagliariello, I.M. Catalano, A. Cingolani, Increase of proton electrochemical potential and ATP synthesis in rat liver mitochondria irradiated in vitro by Helium–Neon laser, *FEBS Lett.* 175 (1984) 95–99.
- [3] Y.L. Jia, Z.Y. Guo, Effect of low-power He–Ne laser irradiation on rabbit articular chondrocytes in vitro, *Lasers Surg. Med.* 34 (2004) 323–328.
- [4] J. Uitto, D. Koura, Cytokine modulation of extracellular matrix gene expression: relevance to fibrotic skin diseases, *J. Dermatol. Sci.* 24 (2000) 60–69.
- [5] L.S. Pugliese, A.P. Medrado, S.R. Reis, Z.A. Andrade, The influence of low-level laser therapy on biomodulation of collagen and elastic fibers, *Pesqui Odontol. Bras.* 17 (2003) 307–313.
- [6] I. Garavello-Freitas, V. Baranauskas, P.P. Joazeiro, C.R. Padovani, M. Dal Pai-Silva, M.A. da Cruz-Hofling, Low-power laser irradiation improves histomorphometrical parameters and bone matrix organization during tibia wound healing in rats, *J. Photochem. Photobiol. B* 70 (2003) 81–89.
- [7] D.T. Fung, G.Y. Ng, M.C. Leung, D.K. Tay, Effects of a therapeutic laser on the ultrastructural morphology of repairing medial collateral ligament in a rat model, *Lasers Surg. Med.* 32 (2003) 286–293.
- [8] J. Tunér, L. Hode, *Laser Therapy in Dentistry and Medicine*, Prima Books, Spjutvägen, 1996.
- [9] A.P. Medrado, L.S. Pugliese, S.R. Reis, Z.A. Andrade, Influence of low level laser therapy on wound healing and its biological action upon myofibroblasts, *Lasers Surg. Med.* 32 (2003) 239–244.
- [10] Z.A. Andrade, J.A. Grimaud, Morphology of chronic collagen resorption. A study on the late stages of schistosomal granuloma involution, *Am. J. Pathol.* 132 (1988) 389–399.
- [11] P.M. do Nascimento, A.L. Pinheiro, M.A.C. Salgado, L. Ramalho, A preliminary report on the effect of laser therapy on the healing of cutaneous surgical wounds as a consequence of an inversely proportional relationship between wavelength and intensity: histological study in rats, *Photomed. Laser Surg.* 22 (2004) 513–518.
- [12] M.J. McCabe, Mechanisms and consequences of silica-induced apoptosis, *Toxicol. Sci.* 76 (2003) 1–2.
- [13] H. Olbrück, N.H. Seemayer, B. Voss, M. Wilhelm, Supernatants from quartz dust treated human macrophages stimulate cell proliferation of different human lung cells as well as collagen-synthesis of human diploid lung fibroblasts in vitro, *Toxicol. Lett.* 96 (1998) 85–95.
- [14] G. Arcangeli, V. Cupelli, G. Giuliano, Effects of silica on human lung fibroblast in culture, *Sci. Total Environ.* 270 (2001) 135–139.
- [15] B. Fubini, A. Hubbard, Reactive oxygen species (ROS) and reactive nitrogen species (RNS) generation by silica in inflammation and fibrosis, *Free Radical Biol. Med.* 34 (2003) 1507–1516.
- [16] A. Giorgio-Miller, S. Bottoms, G. Laurent, P. Carmeliet, S. Herrick, Fibrin-induced skin fibrosis in mice deficient in tissue plasminogen activator, *Am. J. Pathol.* 167 (2005) 721–732.
- [17] B.C. Vidal, M.L.S. Mello, C. Godo, A.C. Caseiro Filho, J.M. Abudaji, Anisotropic properties of silver plus gold-impregnated collagen bundles: ADB and form birefringence curves, *Ann. Histochem.* 20 (1975) 18–26.
- [18] P.C. Bridgman, M.E. Dailey, The organization of myosin and actin in rapid frozen nerve growth cones, *J. Cell Biol.* 108 (1989) 85–109.
- [19] P. Dore-Duff, A. Kataychev, X. Wang, E. Van Buren, CNS microvascular pericytes exhibit multipotential stem cell activity, *J. Cereb. Blood Flow Metab.* 18 (2006) 613–624.
- [20] B. Eyden, The myofibroblast: a study of normal, reactive and neoplastic tissues, with an emphasis on ultrastructure. Part 1 – Normal and reactive cells, *J. Submicrosc. Cytol. Pathol.* 37 (2005) 109–204.
- [21] N. Pourreau-Schneider, A. Ahmed, M. Soudry, J. Acquemier, F. Kopp, J.C. Franquin, P.M. Martin, Helium–Neon laser treatment transforms fibroblasts into myofibroblasts, *Am. J. Pathol.* 137 (1990) 171–178.
- [22] C. Farrington-Rock, N.J. Crofts, M.J. Doherty, B.A. Ashton, C. Griffin-Jones, A.E. Canfield, Chondrogenic and adipogenic potential of microvascular pericytes, *Circulation* 110 (2004) 2226–2232.
- [23] D.J. Rutter, R.O. Schilingemann, J.R. Westphal, E.J.R. Rietveld, R.M.W. de Waa, Angiogenesis in wound healing and tumor metastasis, *Behring Inst. Mitt.* 92 (1993) 258–272.
- [24] A. Schindl, M. Schindl, L. Schindl, W. Jurecka, H. Höningmann, F. Breier, Increased dermal angiogenesis after low-intensity laser therapy for a chronic radiation ulcer determined by a video measuring system, *J. Am. Acad. Dermatol.* 40 (1999) 481–484.
- [25] I. Garavello, V. Baranauskas, M.A. da Cruz-Hofling, The effects of low laser irradiation on angiogenesis in injured rat tibiae, *Histol. Histopathol.* 19 (2004) 43–48.